



Molecular docking studies and biological evaluation of 1,3,4-thiadiazole derivatives bearing Schiff base moieties as tyrosinase inhibitors



Junyuan Tang, Jinbing Liu*, Fengyan Wu

Department of Biology and Chemical Engineering, Shaoyang University, Shao Shui Xi Road, Shaoyang 422100, PR China

ARTICLE INFO

Article history:

Received 30 July 2016

Revised 18 September 2016

Accepted 19 September 2016

Available online 20 September 2016

Keywords:

1,3,4-Thiadiazole derivatives

Tyrosinase inhibitory activities

Inhibition kinetics

Docking studies

ABSTRACT

1,3,4-Thiadiazole derivatives bearing Schiff base moieties were designed, synthesized, and their tyrosinase inhibitory activities were evaluated. Some compounds displayed potent tyrosinase inhibitory activities, especially, 4-(((5-mercapto-1,3,4-thiadiazol-2-yl)-imino)methyl)-2-methoxy-phenol (**14**) exhibited superior inhibitory effect to the other compounds with an IC_{50} value of 0.036 μ M. The structure–activity relationships (SARs) were preliminarily discussed and docking studies showed compound **14** had strong binding affinity to mushroom tyrosinase. Hydroxy might be the active groups. The inhibition kinetics study revealed that compounds (**13** and **14**) inhibited tyrosinase by acting as uncompetitive inhibitors. The LD_{50} value of the compound **14** was 5000 mg/kg.

© 2016 Elsevier Inc. All rights reserved.

1. Introduction

Tyrosinase (monophenol or *o*-diphenol, oxygen oxidoreductase, EC 1.14.18.1, syn. polyphenol oxidase), as known as polyphenol oxidase (PPO) possesses an active site where two copper ions bind dioxygen in a form of the enzyme termed as oxy-tyrosinase [1]. The binuclear center together with three specific histidine residues forms a square-pyramidal structure [2]. Tyrosinase is a key enzyme in the biosynthesis of melanin pigment, and catalyzes two distinct reactions involving molecular oxygen in the hydroxylation of monophenols to *o*-diphenols (monophenolase), as well as oxidation of *o*-diphenols to *o*-quinones (diphenolase) [3]. Therefore, it plays a vital role in the processes of melanin formation in bacteria, fungi, plants and mammals [4]. Because of the high reactivity of tyrosinase, quinones could polymerize spontaneously to form high molecular weight brown-pigments (melanins), which widely spreads in skin, hair and eyes of mammals, or react with amino acids and proteins to enhance brown color of the pigment produced [5]. Although melanin is important in preventing skin cancer caused by overexposure to ultraviolet lights [6,7], excessive melanin production and accumulation may lead to hyperpigmentation such as melasma, freckles, ephelide, and solar lentigines [8]. Tyrosinase is also known to oxidize dopamine to form melanin in the brain, and thus tyrosinase is implicated in the pathogenesis of Parkinson's disease and related neurodegenerative disorders [9,10]. In food industry, tyrosinase catalyzes the reactions resulting

in undesirable browning in fruits, vegetables, and beverages, which impairs the color and sensory properties of these food products and may shorten shelf life, reduce market value, and lose nutritional value during the postharvest handling processes [11]. One way to avoid these negative effects resulted from tyrosinase is to use inhibitors of this enzyme. Furthermore, in insects, tyrosinase is associated with three biochemical processes, including sclerotization of cuticle, defensive encapsulation and melanization of foreign organism, and wound healing [12,13]. These processes provide potential targets for developing safer and effective tyrosinase inhibitors as insecticides and ultimately for insect control. In fact, tyrosinase inhibitors have been well appreciated in the fields of cosmetics, medicine, food sciences and agriculture [14,15]. Most of the recent researches have focused on below following fields: first, finding new naturally occurring inhibitors of tyrosinase; second, proceeding medicinal modifications or synthesis chemical analogs of target inhibitors for better inhibitory activities and lower side effects; third, investigating structure–activity and inhibitory mechanism of tyrosinase inhibitors. By far, some natural and synthetic tyrosinase inhibitors were reported, for example, hydroquinone, ascorbic acid, arbutin, kojic acid, aromatic aldehydes, aromatic acids, aromatic alcohol, tropolone, and polyphenols [16–19]. However, only handful molecules such as kojic acid, arbutin, tropolone, and 1-phenyl-2-thiourea (PTU) are commercially useful [20]. Moreover, it has been reported that arbutin decomposes at room temperature (10% decomposition at 20 °C for 15 days), while arbutin and tropolone have been demonstrated not clinically efficacious when systematically analyzed in carefully controlled studies [21]. As a result, there is still an urgent need for

* Corresponding author.

E-mail address: syuliujb@163.com (J. Liu).

novel tyrosinase inhibitors with higher activity, better pharmacology properties and lower side effect. Gratifyingly, it was reported that phenyl thioureas and alkyl thioureas could exhibit weak to moderate depigmenting activity [22], and the interaction with the hydrophobic protein pocket is close to the binuclear copper active site of tyrosinase. The sulfur atom of in the thioureas can bind to both copper ions in the active site. Similarly, thiosemicarbazide derivatives and curcumin have potential to coordinate the two copper ions in the active site of tyrosinase [23]. Inspired by these precedent literatures, our research provides latest progress in designing tyrosinase inhibitors.

We envisioned that thiadiazole, the hetero sulfur containing aromatic ring, could improve lipophilicity, and the mesoionic nature of thiadiazole makes this class of compounds to show good tissue permeability [24,25]. The two-electron donor nitrogen system ($-N=C-S$) as well as the hydrogen binding domain, may help with pharmacodynamics of the molecule for better binding with the receptors [26]. Plus, thiadiazoles are bioisosteres of pyrimidines, oxadiazoles, oxazoles, benzene and the derivatives have been proved to display diverse range of biological and pharmacological properties [27]. 1,3,4-thiadiazole, a unique structure, represents a key motif in heterocyclic chemistry and medicinal chemistry [28]. For instance, many drugs containing 1,3,4-thiadiazole moieties are available on the market, e.g., acetazolamide, methazolamide and sulfamethazole [29]. Recently, derivatives of 1,3,4-thiadiazole have been reported for their antibacterial, antifungal, inflammatory, antianxiety, and antitubercular activities [30]. Some scientists have studied extensively on 1,3,4-thiadiazole derivatives as potential drugs to treat Alzheimer's disease (AD) [31]. 1,3,4-Thiadiazole derivatives bearing Schiff base moieties even display anticancer, antibacterial, antidepressant, antidiabetic and antifungal activities [32].

Lately, our studies indicated that thiosemicarbazide derivatives exhibited potent inhibitory activities against mushroom tyrosinase. Inhibition mechanism analysis showed that this series of compounds could potentially bind to the binuclear active site of tyrosinase [33]. 1,3,4-Thiadiazole-2(3H)-thiones exhibited potent inhibitory activities against mushroom tyrosinase [34]. But to the best of our knowledge, the tyrosinase inhibitory activities of the 1,3,4-thiadiazole Schiff base derivatives have never been reported in the literatures. Combining the biological significance of 1,3,4-thiadiazole and Schiff base moiety, we designed and synthesized a library of 1,3,4-thiadiazole derivatives bearing Schiff base moieties, and their inhibitory activities against mushroom tyrosinase were evaluated using kojic acid as positive control. The structure–activity relationship (SAR) was analyzed and discussed. To better elucidate the inhibition mechanism, the docking studies were carried out and discussed as well.

2. Materials and methods

2.1. Chemistry

Melting points (m.p.) were determined on SGW-X4 melting point apparatus and the thermometer was uncorrected. NMR spectra were recorded on Bruker 300 spectrometers at 25 °C in DMSO- d_6 using TMS as internal standard for protons. Chemical shift values are mentioned in δ (ppm) and coupling constants (J) are given in Hz. Mass-spectrometric (MS) data is reported in m/z using the LCMS-2010A. The reaction progress was monitored by TLC (Merck Kieselgel 60 F254). The chromatograms were visualized under UV 254–365 nm and iodine. Infrared (IR) spectra were recorded on VECTOR 22 spectrometer in KBr pellets and are reported in cm^{-1} . Tyrosinase, L-3,4-dihydroxyphenylalanine (L-DOPA) and kojic acid were purchased from Sigma–Aldrich Chemical Co (Shanghai,

China). Other chemicals were purchased from commercial suppliers and were used without further purification.

2.1.1. Synthesis of 1,3,4-thiadiazole derivatives bearing Schiff base moieties [30,35]

Thiosemicarbazide 18.228 g (0.2 mol) and anhydrous sodium carbonate 10.6 g (0.1 mol) were suspended in 80 mL anhydrous ethanol. The reaction mixture was stirred at RT and carbon disulphide 0.2 mol (15.228 g) was added dropwise in 1 h. The reaction mixture was stirred under reflux for 4 h and monitored by TLC until the reaction was completed. After completion of reaction, the mixture was allowed to cool to room temperature, water (100 mL) was then added to the mixture and neutralized by the 10% solution of hydrochloric acid, white precipitates of 2-amino-5-mercapto-1,3,4-thiadiazole were generated.

2-Amino-5-mercapto-1,3,4-thiadiazole (5 mmol) was suspended in 10 mL anhydrous ethanol and 6 mmol of different aromatic aldehyde was added, using three drops concentrated sulfuric acid as catalyst. The reaction mixture was stirred under reflux for 8 h and monitored by TLC until the reaction was completed. After completion of reaction, the mixture was allowed to cool to room temperature, and then left overnight. Precipitates of 1,3,4-thiadiazole derivatives bearing Schiff base moieties were generated. The solids were filtered, and washed with the mixture of ethanol and hot water (1:1); dried solid was purified by crystallization from anhydrous alcohol to afford the desired compound.

2.1.1.1. *2-(Benzylideneamino)-5-mercapto-1,3,4-thiadiazole (1)*. Yield 51.4%. Yellow solid, mp: 237–239.2 °C, IR (KBr) ν_{max} 3310, 1567, 1476, 1376, 1312, 1121, 1051, 749, 711 cm^{-1} ; 1H NMR (DMSO- d_6 , 300 MHz) δ 13.02 (s, 1H, SH), 8.62 (s, 1H, =CH), 7.91 (d, 2H, J = 8.7 Hz, ph-H), 7.60 (t, 1H, J = 7.5 Hz, ph-H), 7.45 (t, 2H, J = 7.5 Hz, ph-H); ^{13}C NMR (DMSO- d_6 , 75 MHz) δ 193.1, 180.9, 161.4, 136.1, 133.7, 129.9, 128.6; MS (ESI): m/z (100%) 222 (M^+); Anal. Calcd for $C_9H_7N_3S_2$: C, 48.85; H, 3.19; N, 18.99; found: C, 48.82; H, 3.18; N, 18.96.

2.1.1.2. *2-((2-Fluorobenzylidene)amino)-5-mercapto-1,3,4-thiadiazole (2)*. Yield 16%. Yellow solid, mp: 242.6–244.1 °C, IR (KBr) ν_{max} 3223, 2995, 1562, 1491, 1382, 1313, 1267, 1208, 1108, 1051, 942, 754, 671 cm^{-1} ; 1H NMR (DMSO- d_6 , 300 MHz) δ 13.18 (s, 1H, SH), 8.83 (s, 1H, =CH), 8.25 (d, 1H, J = 7.5 Hz, ph-H), 7.54 (t, 1H, J = 8.1 Hz, ph-H), 7.34 (d, 1H, J = 7.5 Hz, ph-H), 7.29 (t, 1H, J = 8.1 Hz, ph-H); ^{13}C NMR (DMSO- d_6 , 75 MHz) δ 187.9, 180.8, 157.4, 136.9, 131.7, 129.4, 125.2, 122.1, 116.8; MS (ESI): m/z (100%) 240 (M^+); Anal. Calcd for $C_9H_6FN_3S_2$: C, 45.17; H, 2.53; N, 17.56; found: C, 45.15; H, 2.53; N, 17.52.

2.1.1.3. *2-((3-Chlorobenzylidene)amino)-5-mercapto-1,3,4-thiadiazole (3)*. Yield 59.9%. Yellow solid, mp: 253.4–255.3 °C, IR (KBr) ν_{max} 3284, 1570, 1510, 1373, 1309, 1259, 1188, 1105, 1047, 738, 677 cm^{-1} ; 1H NMR (DMSO- d_6 , 300 MHz) δ 13.12 (s, 1H, SH), 8.86 (s, 1H, =CH), 8.12 (s, 1H, ph-H), 7.96 (d, 1H, J = 7.8 Hz, ph-H), 7.80 (d, 1H, J = 6.9 Hz, ph-H), 7.45 (t, 1H, J = 8.7 Hz, ph-H); ^{13}C NMR (DMSO- d_6 , 75 MHz) δ 192.1, 180.5, 161.4, 136.5, 134.2, 131.2, 130.4, 127.9, 127.0; MS (ESI): m/z (100%) 256 (M^+); Anal. Calcd for $C_9H_6ClN_3S_2$: C, 42.27; H, 2.36; N, 16.43; found: C, 42.25; H, 2.35; N, 16.42.

2.1.1.4. *2-((4-Chlorobenzylidene)amino)-5-mercapto-1,3,4-thiadiazole (4)*. Yield 30.2%. Yellow solid, mp: 222.1–224.5 °C, IR (KBr) ν_{max} 3275, 1563, 1488, 1376, 1313, 1259, 1185, 1094, 1051, 1015, 783, 744 cm^{-1} ; 1H NMR (DMSO- d_6 , 300 MHz) δ 13.18 (s, 1H, SH), 8.75 (s, 1H, =CH), 7.95 (d, 2H, J = 6.9 Hz, ph-H), 7.71 (d, 2H, J = 6.9 Hz, ph-H); ^{13}C NMR (DMSO- d_6 , 75 MHz) δ 192.1, 180.9, 161.4, 139.3, 134.8, 131.5, 129.3; MS (ESI): m/z (100%) 256 (M^+);

Anal. Calcd for $C_9H_6ClN_3S_2$: C, 42.27; H, 2.36; N, 16.43; found: C, 42.28; H, 2.34; N, 16.45.

2.1.1.5. 2-((3,4-Dichlorobenzylidene)amino)-5-mercapto-1,3,4-thiadiazole (5). Yield 67.8%. Yellow solid, mp: 223.3–225.7 °C, IR (KBr) ν_{\max} 3404, 1566, 1469, 1376, 1309, 1264, 1190, 1103, 1053, 746, 667 cm^{-1} ; 1H NMR (DMSO- d_6 , 300 MHz) δ 13.15 (s, 1H, SH), 8.82 (s, 1H, =CH), 7.97 (s, 1H, ph-H), 7.75 (d, 1H, J = 8.4 Hz, ph-H), 7.65 (d, 1H, J = 8.4 Hz, ph-H); ^{13}C NMR (DMSO- d_6 , 75 MHz) δ 189.7, 181.3, 159.8, 136.8, 135.1, 134.5, 133.2, 131.3, 128.4; MS (ESI): m/z (100%) 291 (M^+); Anal. Calcd for $C_9H_5Cl_2N_3S_2$: C, 37.25; H, 1.74; N, 14.48; found: C, 37.28; H, 1.76; N, 14.49.

2.1.1.6. 4-Chloro-2-(((5-mercapto-1,3,4-thiadiazol-2-yl)imino)methyl)phenol (6). Yield 53%. Yellow solid, mp: 247.3–250.1 °C, IR (KBr) ν_{\max} 3440, 3067, 2862, 1599, 1561, 1517, 1470, 1231, 1173, 1063, 804, 711 cm^{-1} ; 1H NMR (DMSO- d_6 , 300 MHz) δ 14.58 (s, 1H, SH), 11.27 (s, 1H, OH), 8.80 (s, 1H, =CH), 7.84 (s, 1H, ph-H), 7.54 (d, 1H, J = 8.7 Hz, ph-H), 7.05 (d, 1H, J = 8.7 Hz, ph-H); ^{13}C NMR (DMSO- d_6 , 75 MHz) δ 189.7, 180.7, 164.0, 158.7, 135.0, 127.8, 123.6, 121.1, 119.5; MS (ESI): m/z (100%) 272 (M^+); Anal. Calcd for $C_9H_6ClN_3OS_2$: C, 39.78; H, 2.23; N, 15.46; found: C, 39.76; H, 2.25; N, 15.48.

2.1.1.7. 4-Bromo-2-(((5-mercapto-1,3,4-thiadiazol-2-yl)imino)methyl)phenol (7). Yield 51.5%. Yellow solid, mp: 253.0–255.1 °C, IR (KBr) ν_{\max} 3420, 3058, 2858, 1606, 1555, 1512, 1467, 1347, 1269, 1171, 1062, 965, 828, 729 cm^{-1} ; 1H NMR (DMSO- d_6 , 300 MHz) δ 14.57 (s, 1H, SH), 11.28 (s, 1H, OH), 8.78 (s, 1H, =CH), 7.97 (s, 1H, ph-H), 7.61 (d, 1H, J = 8.7 Hz, ph-H), 7.00 (d, 1H, J = 8.7 Hz, ph-H); ^{13}C NMR (DMSO- d_6 , 75 MHz) δ 189.6, 180.7, 163.9, 159.3, 137.7, 130.9, 124.2, 121.7, 110.9; MS (ESI): m/z (100%) 317 (M^+); Anal. Calcd for $C_9H_6BrN_3OS_2$: C, 34.19; H, 1.91; N, 13.29; found: C, 34.18; H, 1.93; N, 13.32.

2.1.1.8. 2-((4-(Tert-butyl)benzylidene)amino)-5-mercapto-1,3,4-thiadiazole (8). Yield 66.1%. White solid, mp 214.2–216.5 °C, IR (KBr) ν_{\max} 3395, 2960, 2868, 1689, 1607, 1567, 1499, 1379, 1315, 1264, 1185, 1105, 1052, 931, 835, 761 cm^{-1} ; 1H NMR (DMSO- d_6 , 300 MHz) δ 13.25 (s, 1H, SH), 8.83 (s, 1H, =CH), 7.66 (d, 2H, J = 8.4 Hz, ph-H), 7.48 (d, 2H, J = 8.4 Hz, ph-H), 1.35 (s, 9H, 3CH₃); ^{13}C NMR (DMSO- d_6 , 75 MHz) δ 192.2, 180.7, 155.7, 152.9, 131.3, 129.7, 126.8, 34.8, 31.2; MS (ESI): m/z (100%) 278 (M^+); Anal. Calcd for $C_{13}H_{15}N_3S_2$: C, 56.28; H, 5.45; N, 15.15; found: C, 56.29; H, 5.44; N, 15.12.

2.1.1.9. 2-((2-Nitrobenzylidene)amino)-5-mercapto-1,3,4-thiadiazole (9). Yield 22.7%. Yellow solid, mp: 229.7–232.2 °C, IR (KBr) ν_{\max} 3221, 2987, 1610, 1562, 1519, 1352, 1309, 1265, 1215, 1188, 1110, 1055, 947, 856, 781, 733 cm^{-1} ; 1H NMR (DMSO- d_6 , 300 MHz) δ 13.19 (s, 1H, SH), 9.36 (s, 1H, =CH), 8.16 (d, 1H, J = 8.1 Hz, ph-H), 7.92 (d, 1H, J = 7.5 Hz, ph-H), 7.79 (t, 1H, J = 8.4 Hz, ph-H), 7.67 (t, 1H, J = 7.8 Hz, ph-H); ^{13}C NMR (DMSO- d_6 , 75 MHz) δ 189.9, 180.1, 158.6, 149.5, 134.2, 133.7, 130.8, 128.2, 124.9; MS (ESI): m/z (100%) 267 (M^+); Anal. Calcd for $C_9H_6N_4O_2S_2$: C, 40.59; H, 2.27; N, 21.04; found: C, 40.58; H, 2.28; N, 21.06.

2.1.1.10. 2-((2-Methoxybenzylidene)amino)-5-mercapto-1,3,4-thiadiazole (10). Yield 38.3%. Yellow solid, mp: 148.2–151.3 °C, IR (KBr) ν_{\max} 3328, 2934, 2835, 1564, 1491, 1373, 1312, 1252, 1175, 1116, 1051, 933, 802, 754 cm^{-1} ; 1H NMR (DMSO- d_6 , 300 MHz) δ 13.17 (s, 1H, SH), 9.32 (s, 1H, =CH), 7.69 (d, 1H, J = 8.1 Hz, ph-H), 7.52 (t, 1H, J = 8.4 Hz, ph-H), 7.03 (d, 1H, J = 8.4 Hz, ph-H), 6.99 (t, 1H, J = 7.8 Hz, ph-H); ^{13}C NMR (DMSO- d_6 , 75 MHz) δ 189.9, 181.2, 157.4, 155.5, 135.9, 131.0, 128.6, 122.4, 121.0, 56.0; MS (ESI): m/z (100%) 252 (M^+); Anal. Calcd for $C_{10}H_9N_3OS_2$: C, 47.79; H, 3.61; N, 16.72; found: C, 47.82; H, 3.63; N, 16.75.

2.1.1.11. 2-((3,5-Dimethoxybenzylidene)amino)-5-mercapto-1,3,4-thiadiazole (11). Yield 44.8%. Yellow solid, mp: 227–229 °C, IR (KBr) ν_{\max} 3339, 3082, 2926, 1609, 1557, 1463, 1325, 1264, 1200, 1155, 1059, 971, 845, 754 cm^{-1} ; 1H NMR (DMSO- d_6 , 300 MHz) δ 13.19 (s, 1H, SH), 8.67 (s, 1H, =CH), 7.08 (s, 2H, ph-H), 6.61 (s, 1H, ph-H), 3.76 (s, 6H, 2CH₃); ^{13}C NMR (DMSO- d_6 , 75 MHz) δ 186.8, 180.9, 168.7, 161.4, 138.7, 107.5, 104.2, 55.58; MS (ESI): m/z (100%) 282 (M^+); Anal. Calcd for $C_{11}H_{11}N_3O_3S_2$: C, 46.96; H, 3.94; N, 14.93; found: C, 46.95; H, 3.96; N, 14.97.

2.1.1.12. 2-(((5-Mercapto-1,3,4-thiadiazol-2-yl)imino)methyl)phenol (12). Yield 51%. Yellow solid, mp: 252–254 °C, IR (KBr) ν_{\max} 3434, 3072, 2875, 1607, 1571, 1528, 1482, 1374, 1276, 1199, 1146, 1067, 761 cm^{-1} ; 1H NMR (DMSO- d_6 , 300 MHz) δ 14.53 (s, 1H, SH), 11.15 (s, 1H, OH), 8.88 (s, 1H, =CH), 7.87 (d, 1H, J = 7.8 Hz, ph-H), 7.53 (t, 1H, J = 7.2 Hz, ph-H), 7.02–6.96 (m, 2H, ph-H); ^{13}C NMR (DMSO- d_6 , 75 MHz) δ 191.7, 186.5, 166.1, 160.8, 135.8, 130.1, 119.9, 119.5, 117.2; MS (ESI): m/z (100%) 238 (M^+); Anal. Calcd for $C_9H_7N_3OS_2$: C, 45.55; H, 2.97; N, 17.71; found: C, 45.57; H, 2.98; N, 17.73.

2.1.1.13. 4-(((5-Mercapto-1,3,4-thiadiazol-2-yl)imino)methyl)benzene-1,3-diol (13). Yield 57.6%. Yellow solid, mp: 240–243 °C, IR (KBr) ν_{\max} 3305, 3139, 1635, 1587, 1516, 1438, 1319, 1241, 1213, 1171, 1113, 1059, 973, 864, 797 cm^{-1} ; 1H NMR (DMSO- d_6 , 300 MHz) δ 14.37 (s, 1H, SH), 11.40 (s, 1H, OH), 10.73 (s, 1H, OH), 8.70 (s, 1H, =CH), 7.71 (d, 1H, J = 6.9 Hz, ph-H), 7.65 (s, 1H, ph-H), 6.34 (d, 1H, J = 6.9 Hz, ph-H); ^{13}C NMR (DMSO- d_6 , 75 MHz) δ 190.9, 185.9, 165.7, 164.4, 163.2, 133.2, 119.9, 109.3, 102.3; MS (ESI): m/z (100%) 254 (M^+); Anal. Calcd for $C_9H_7N_3O_2S_2$: C, 42.68; H, 2.79; N, 16.59; found: C, 42.66; H, 2.82; N, 16.57.

2.1.1.14. 4-(((5-Mercapto-1,3,4-thiadiazol-2-yl)imino)methyl)-2-methoxyphenol (14). Yield 63.2%. Yellow solid, mp: 219.5–221.8 °C, IR (KBr) ν_{\max} 3275, 1606, 1565, 1512, 1382, 1322, 1272, 1205, 1101, 1053, 928, 753 cm^{-1} ; 1H NMR (DMSO- d_6 , 300 MHz) δ 14.41 (s, 1H, SH), 10.34 (s, 1H, OH), 8.55 (s, 1H, =CH), 7.55 (s, 1H, ph-H), 7.42 (d, 1H, J = 8.7 Hz, ph-H), 6.99 (d, 1H, J = 8.7 Hz, ph-H), 3.86 (s, 3H, CH₃); ^{13}C NMR (DMSO- d_6 , 75 MHz) δ 190.9, 186.2, 167.9, 152.9, 148.1, 128.6, 126.7, 115.6, 111.1, 55.5; MS (ESI): m/z (100%) 268 (M^+); Anal. Calcd for $C_{10}H_9N_3O_2S_2$: C, 44.93; H, 3.39; N, 15.72; found: C, 44.96; H, 3.38; N, 15.73.

2.1.1.15. 4-(((5-Mercapto-1,3,4-thiadiazol-2-yl)imino)methyl)-2,6-dimethoxyphenol (15). Yield 52.2%. Yellow solid, mp: 267–268.5 °C, 1H NMR (DMSO- d_6 , 300 MHz) δ 14.42 (s, 1H, SH), 9.77 (s, 1H, OH), 8.53 (s, 1H, =CH), 7.31 (s, 2H, ph-H), 3.84 (s, 6H, 2CH₃); ^{13}C NMR (DMSO- d_6 , 75 MHz) δ 191.1, 186.0, 168.1, 148.1, 142.0, 124.4, 107.6, 56.2; MS (ESI): m/z (100%) 298 (M^+); Anal. Calcd for $C_{11}H_{11}N_3O_3S_2$: C, 44.43; H, 3.73; N, 14.13; found: C, 44.45; H, 3.76; N, 14.13.

2.1.1.16. 2-((2,4,6-Trimethoxybenzylidene)amino)-5-mercapto-1,3,4-thiadiazole (16). Yield 86%. Yellow solid, mp: 263–265 °C, IR (KBr) ν_{\max} 3084, 2890, 1599, 1520, 1463, 1384, 1325, 1276, 1239, 1113, 1064, 767 cm^{-1} ; 1H NMR (DMSO- d_6 , 300 MHz) δ 14.29 (s, 1H, SH), 8.69 (s, 1H, =CH), 6.31 (s, 2H, ph-H), 3.90 (s, 6H, 2CH₃), 3.82 (s, 3H, CH₃); ^{13}C NMR (DMSO- d_6 , 75 MHz) δ 190.8, 185.8, 167.2, 163.4, 161.3, 104.5, 91.7, 56.3, 55.7; MS (ESI): m/z (100%) 312 (M^+); Anal. Calcd for $C_{12}H_{13}N_3O_3S_2$: C, 46.29; H, 4.21; N, 13.49; found: C, 46.31; H, 4.23; N, 13.52.

2.1.1.17. 2-(((5-(Benzylthio)-1,3,4-thiadiazol-2-yl)imino)methyl)-4-chlorophenol (17). 2-Amino-5-mercapto-1,3,4-thiadiazole 3.99 g (0.03 mol) was added to a 50 mL flask, and the solution of KOH (1.683 g, 0.03 mol) in 10 mL was added under stirring at room

temperature. Halogenated hydrocarbon (0.1 mol) was added by dropwise in 0.5 h with vigorous stirring. The reaction mixture was stirred at room temperature and checked by TLC (petroleum ether: ethyl acetate 1:1). When reaction was complete, the yellow precipitate of crude thiadiazole sulfide was formed. This was filtered, washed with water to neutrality, and crystallized from 95% ethanol.

2-Amino-5-sulfide-1,3,4-thiadiazole (5 mmol) was suspended in 10 mL anhydrous ethanol and 6 mmol of aromatic aldehyde was added, using tetrabutylammonium bromide (TBAB) as catalyst. The reaction mixture was stirred under reflux for 8 h and monitored by TLC (petroleum ether: ethyl acetate 4:1) until the reaction was complete. After completion of reaction, the mixture was allowed to cool to room temperature, and then left overnight. Precipitates of 1,3,4-thiadiazole sulfide derivative bearing Schiff base moieties were produced. The solid that separated out was filtered, washed with the mixture of ethanol and hot water (1:1); dried solid was purified by crystallization from anhydrous alcohol to afford the desired compound.

Yield 49.92%. Yellow solid, mp: 148.2–150.7 °C, ^1H NMR (CDCl_3 , 500 MHz) δ 11.79 (s, 1H, OH), 8.95 (s, 1H, CH), 7.44–7.30 (m, 7H, Ph-H), 7.00 (d, $J = 8.6$ Hz, 1H, Ph-H), 4.57 (s, 2H, CH_2); ^{13}C NMR (CDCl_3 , 125 MHz) δ 170.4, 166.7, 164.8, 160.2, 135.6, 132.6, 132.3, 129.3, 128.9, 128.1, 124.6, 119.4, 118.9, 38.4; MS (ESI): m/z (100%) 362 (M^+). Anal. Calcd for $\text{C}_{16}\text{H}_{12}\text{ClN}_3\text{OS}_2$: C, 53.11; H, 3.34; N, 11.61; found: C, 53.09; H, 3.36; N, 11.63.

2.2. Tyrosinase activity assay

Tyrosinase inhibition assays were performed according to the method reported by our group [36]. Briefly, 1,3,4-thiadiazole derivatives were tested for diphenolase inhibitory activity of tyrosinase using L-DOPA (dihydroxyphenylalanine) as substrate. All the compounds were dissolved in DMSO and its final concentration in the reaction mixture was 2.0%. Thirty units of mushroom tyrosinase (0.5 mg/ml) were first pre-incubated with the compounds, in 50 mM phosphate buffer (pH 6.8), for 10 min at 25 °C. Then the L-DOPA (0.5 mM) was added to the reaction mixture and the enzyme reaction was continuously monitored by measuring the change in absorbance at 475 nm of formation of the DOPA chrome for 1 min. The measurement was performed in triplicate for each concentration and averaged before further calculation. The activity was expressed as the sample concentration that gave a 50% inhibition in the enzyme activity (IC_{50}). The percent of inhibition of tyrosinase was calculated as follows:

$$\text{Inhibition rate (\%)} = [(B - S)/B] \times 100$$

Here, the B and S were the absorbances for the blank and samples. All the experiments were carried out at least in triplicate and averaged. Kojic acid was used as the positive control.

2.3. Kinetic analysis of the inhibition of tyrosinase

A series of experiments were performed to determine the inhibition kinetics by following method [37]. Inhibitor (**13**) with concentrations 0, 0.025, 0.05, 0.075, 0.1 μM , and (**14**) with concentrations 0, 0.005, 0.01, 0.015 and 0.02 μM , respectively were used. Substrate L-DOPA concentration was among 1014–304 μM in all kinetic study. Preincubation and measurement time was the same as discussed in mushroom tyrosinase inhibition assay protocol. The inhibition type on the enzyme was assayed by Lineweaver Burk plots of inverse of velocities ($1/V$) versus inverse of substrate concentration $1/[S]$ mM^{-1} , and the inhibition constants were determined by the secondary plots of the apparent $1/V_m$ versus the concentrations of the inhibitors.

2.4. In silico docking simulation of tyrosinase with compounds 14 [38–40]

For docking simulations, we used the AutoDock4.2 program. Among the many tools available for in silico protein-ligand docking, AutoDock4.2 is the most commonly used due to its automated docking capability. The 3D structure of tyrosinase was used the crystal structure of *Agaricus bisporus* (PDB ID: 2Y9X) without homology modeling. We conducted simulations of the docking of tyrosinase to the compounds **14**. To prepare the compound for the docking simulation, the following steps was performed: (1) conversion of 2D structures into 3D structures, (2) calculation of charges, and (3) addition of hydrogen atoms using the ChemOffice program (<http://www.cambridgeoft.com>).

2.5. Acute toxicity [41]

Acute toxicity experiments were carried out using KM mice of both sexes weighing 18–22 g. The food and water were provided according to EPA OPPTS Harmonized Test guideline. All animals were provided by Qinlongshan Laboratory animal center SCXK (Yu) 2005-0001. Various doses of the compound **14** were given by intragastric administration to the healthy KM mice. After the intragastric administration of the compound, mice were observed continuously for any gross behavioral changes and deaths, and intermittently for 1 week, the LD_{50} values can be obtained.

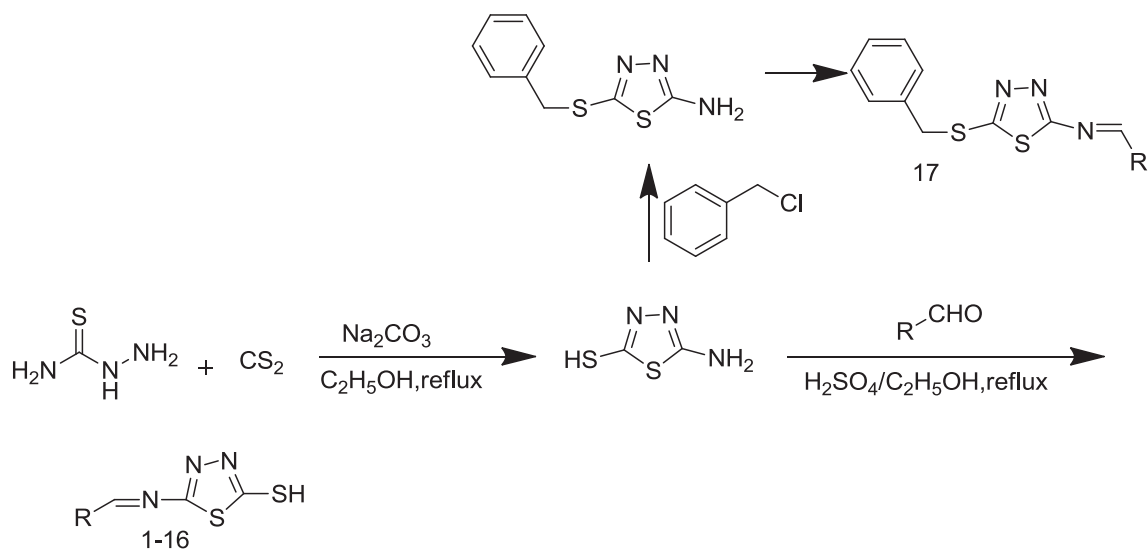
3. Results and discussion

3.1. Chemistry

The synthesis of 1,3,4-thiadiazole derivatives was shown in Scheme 1. As depicted in Scheme 1, 2-amino-5-mercapto-1,3,4-thiadiazole can be synthesized by the condensation reaction of thiosemicarbazide with carbon disulphide in ethanol using anhydrous sodium carbonate as catalyst under reflux conditions. Thiadiazole sulfide was synthesized from 2-amino-5-mercapto-1,3,4-thiadiazole and halogenated hydrocarbon. 1,3,4-thiadiazole derivatives bearing Schiff base moieties were prepared by condensing 2-amino-5-mercapto-1,3,4-thiadiazole or 5-(benzylamino)-1,3,4-thiadiazole-2-thiol with different aromatic aldehydes in ethanol using concentrated sulfuric acid as catalyst under reflux conditions. The resulting products were obtained in moderate yields. All the target compounds were characterized spectroscopic methods.

3.2. Biological activity

The **17** synthesized compounds were assessed using tyrosinase inhibition assay with kojic acid as a positive control, and the IC_{50} values against tyrosinase were recorded in Table 1. As we expected, **15** compounds exhibited potent inhibition activities against mushroom tyrosinase, with IC_{50} values at single digit or sub-micromolar level, better than the reference inhibitor kojic acid. The other compounds showed some inhibitory activities against tyrosinase. Pleasingly, compound **14** exhibited the most potent tyrosinase inhibitory activity with IC_{50} value of 0.036 μM . The results showed that the substitution pattern of the benzene ring has a great influence in determining activities against tyrosinase. From the result of Table 1, if the hydrogens on benzene ring were substituted with halogens, all of the compounds showed better inhibitory activities than compound **1** (49.246 μM). Compound **3** exhibited lower inhibitory activity than compound **4**. However, the dihalogen substituted compound **5** showed lower inhibitory activity than the compound **4**. The results showed that the type, position and



1. R = phenyl;
2. R = 2-fluorophenyl;
3. R = 3-chlorophenyl;
4. R = 4-chlorophenyl;
5. R = 3,4-dichlorophenyl;
6. R = 5-chloro-2-hydroxyphenyl;
7. R = 5-bromo-2-hydroxyphenyl;
8. R = 4-t-Bu-phenyl;
9. R = 2-nitrophenyl;
10. R = 2-methoxyphenyl;
11. R = 3,5-dimethoxyphenyl;
12. R = 2-hydroxyphenyl;
13. R = 2,4-dihydroxyphenyl;
14. R = 4-hydroxy-3-methoxyphenyl;
15. R = 3,5-dimethoxy-4-hydroxyphenyl;
16. R = 2,4,6-trimethoxyphenyl;
17. R = 5-chloro-2-hydroxyphenyl.

Scheme 1. The synthesis of 1,3,4-thiadiazole derivatives bearing Schiff base moieties.

Table 1
Tyrosinase inhibitory activities of the synthesized compounds.

Compounds	R	IC ₅₀ (μM) ^a ± SD
1	Phenyl	49.246 ± 0.184
2	2-Fluorophenyl	0.765 ± 0.077
3	3-Chlorophenyl	4.753 ± 0.109
4	4-Chlorophenyl	2.460 ± 0.155
5	3,4-Dichlorophenyl	3.621 ± 0.142
6	5-Chloro-2-hydroxyphenyl	1.718 ± 0.135
7	5-Bromo-2-hydroxyphenyl	1.971 ± 0.131
8	4-Bu-phenyl	1.390 ± 0.118
9	2-Nitrophenyl	0.671 ± 0.093
10	2-Methoxyphenyl	0.733 ± 0.083
11	3,5-Dimethoxyphenyl	5.353 ± 0.136
12	2-Hydroxyphenyl	0.785 ± 0.064
13	2,4-Dihydroxyphenyl	0.255 ± 0.065
14	4-Hydroxy-3-methoxyphenyl	0.036 ± 0.002
15	3,5-Dimethoxy-4-hydroxyphenyl	0.473 ± 0.096
16	2,4,6-Trimethoxyphenyl	0.907 ± 0.142
17	5-Chloro-2-hydroxyphenyl	247.350 ± 3.782
Kojic acid	-	23.6

^a Inhibitor concentration (mean of three independent experiments) required for 50% inactivation of tyrosinase.

number of halogen atom at the benzene ring might modulate the activities. When the hydrogen of benzene ring was replaced by flu-

orine, better inhibitory activity was achieved than other halogen substituted compounds. The IC₅₀ value of compound **2** was 0.765 μM, the IC₅₀ values of the two compounds **3** and **4** were 4.753 μM and 2.460 μM, respectively. This result may be because fluorine atom has smaller atomic radius and greater electronegativity. Moreover, comparing to the tyrosinase inhibitory activity of compounds **3**, **4** and **6**, when the hydroxyl group was introduced onto the benzene ring, an elevated inhibitory activity could be observed. These results showed that hydroxyl group may be beneficial to increasing the inhibitory activity of this kind of compounds with halogen atom at benzene ring. From [Table 1](#), the IC₅₀ value of compound **10** with a methoxyl substituted benzene ring (2-position) was 0.733 μM. However, compound **11** with disubstituted methoxyl groups (3,5-position) exhibited some tyrosinase inhibitory activity with an IC₅₀ value of 5.353 μM, it showed lower inhibitory activity than the compound **10**. Interestingly, the IC₅₀ of compound **16** with trisubstituted methoxyl groups (2,4,6-position) was 0.907 μM. This result might be explained that the inhibitory activity methoxyl substituted compound might be related to the position of methoxyl group.

For compounds **12** and **13**, the inhibitory activity increased as the number of hydroxyl group increased. This result showed the hydroxyl group number might have some influences on the inhibitory activity. Compound **14** was the best inhibitor among all the

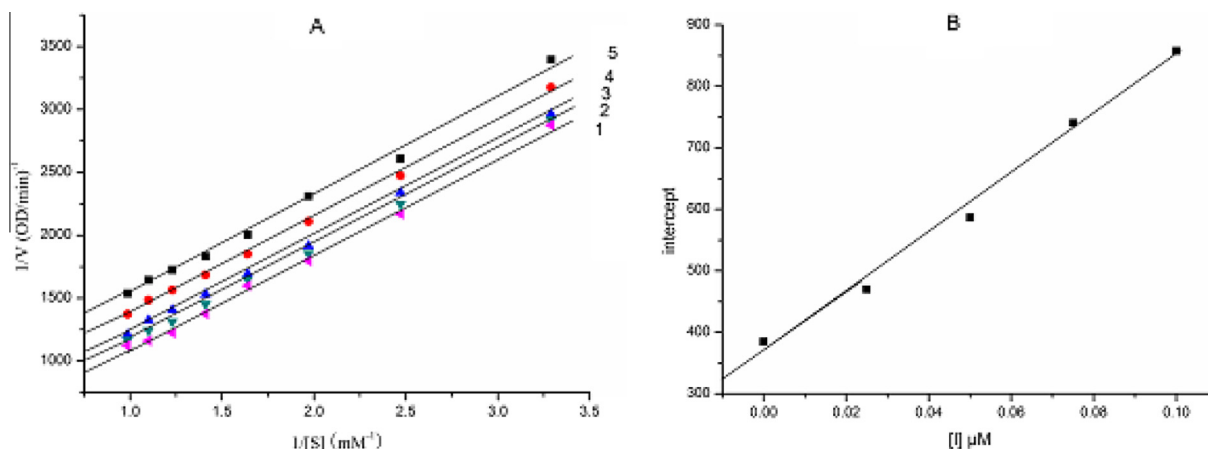


Fig. 1. (A) Kinetic inhibition analysis of compound **13** against the oxidation of L-DOPA by tyrosinase. The mode of inhibition type exhibited through Lineweaver-Burk plot with different concentrations of compound **13**. The inhibitor concentrations of compound **13** for Curves 1–5 were 0, 0.025, 0.05, 0.075 and 0.1 μM . (B) The plot of intercept versus concentration of compound **13** was used to determine the inhibition constant K_i .

compounds, but in contrast, with the increased number of the methoxyl groups, the inhibitory activity of the compound **15** was decreased. This result might be related to the steric hindrance. However, compound **15** exhibited better inhibitory activity than the compound **11**. The result also showed that hydroxyl group may be beneficial to increasing the inhibitory activity. From the Table 1, based on the inhibitory activity of compounds **6** and **17**, when the thiol group was etherified by the benzyl chloride, the inhibitory activity dropped drastically. Thus, free thiol group could be an active group in the inhibition. In addition, the o-dopaquinone can react with the thiol group of the inhibitor [42].

3.3. Inhibitory mechanism

Among the tested target compounds, compound **13** and **14** showed superior inhibitory activities to the other compounds, and therefore, we carried out the kinetic analysis of the two compounds for tyrosinase inhibition using L-DOPA as the substrate. The Lineweaver–Burk plots for the inhibition of tyrosinase by the two compounds and the substrate (Figs. 1 and 2). The inhibition types on the enzyme by compounds **13** and **14** for oxidation of LDOPA were studied as shown in Figs. 1 and 2, respectively. The plots of $1/v$ versus $1/[S]$ gave a family of parallel straight lines

with the same slopes. Meanwhile, as the inhibitor concentration increased, the values of both k_m and V_m decreased, but the ratio of k_m/V_m remained unchanged. The results indicated that both

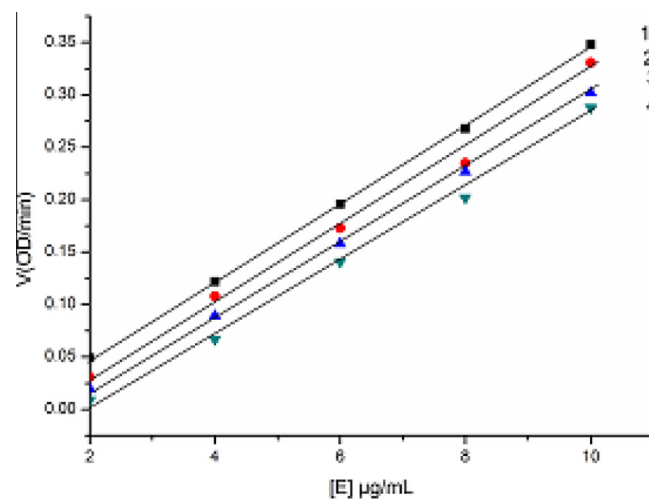


Fig. 3. The effect of concentrations of tyrosinase on its activity for the catalysis of L-DOPA at different concentration of compound **9**. The concentrations of compound **9** for curves 1–4 are 0, 0.25, 0.5 and 1 μM , respectively.

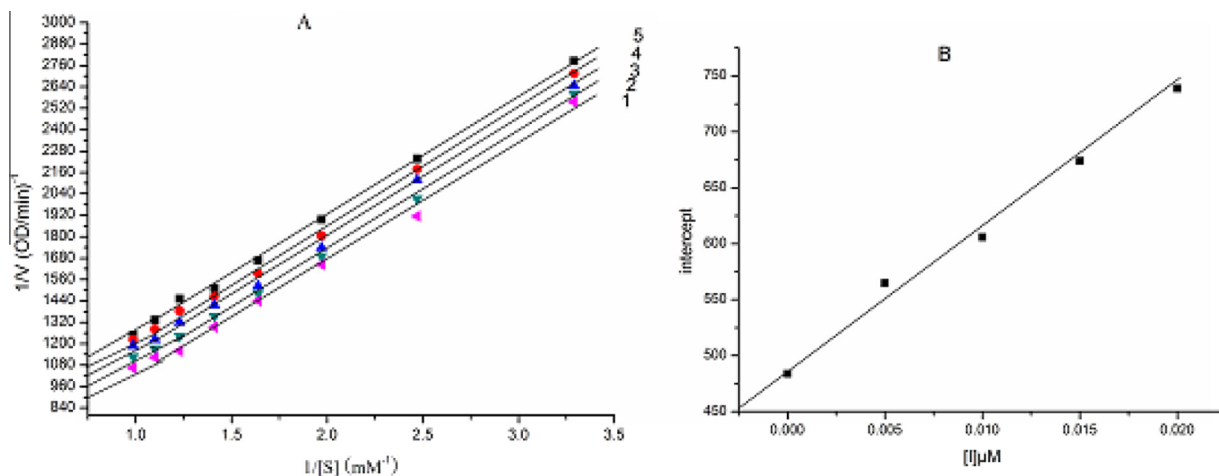


Fig. 2. (A) Kinetic inhibition analysis of compound **14** against the oxidation of L-DOPA by tyrosinase. The mode of inhibition type exhibited through Lineweaver-Burk plot with different concentrations of compound **14**. The inhibitor concentrations of compound **14** for Curves 1–5 were 0, 0.005, 0.01, 0.015 and 0.02 μM . (B) The plot of intercept versus concentration of compound **14** was used to determine the inhibition constant K_i .

compounds **13** and **14** were uncompetitive inhibitors. The inhibition constants (K_i) of the two compounds **13** and **14** were obtained from a plot of the vertical intercept ($1/V_m$) versus the concentration of the inhibitors as $0.075 \mu\text{M}$ and $0.038 \mu\text{M}$, respectively. The catalytic constants (k_{cat}) of the two compounds **13** and **14** were 0.61 s^{-1} and 0.83 s^{-1} . k_{cat}/K_m values of the two compounds **13** and **14** were $1.27 \text{ mM}^{-1} \text{ s}^{-1}$ and $1.08 \text{ mM}^{-1} \text{ s}^{-1}$. The inhibitory mechanism of the compound **9** with no hydroxyl group on mushroom tyrosinase for the oxidation of L-DOPA was determined (Fig. 3). The result displayed that the plots of V versus $[E]$ gave a family of parallel straight lines with the same slopes, thus compound **9** was irreversible inhibitor.

3.4. In silico docking between tyrosinase and compounds 14

The binding affinities of the inhibitors to the receptor tyrosinase were calculated using computational docking studies. The lower value showed the more stable complex formed between the ligand and target protein. The binding energy of compound **14** was

-5.94 kcal/mol , it proved that compound **14** formed stable drug receptor complex with tyrosinase. The phenolic hydroxyl present at position 4 in compound **14** can interact with the copper atom (Cu 401) of tyrosinase (Fig. 4). This result showed hydroxyl group might be activity group. Van der Waals force is also the interaction between compound **14** and tyrosinase. The 1,3,4-thiadiazole ring formed pi-lone pair to GLY281 with bond length of 2.91 \AA . The π - π stacking present in the compound **14** between phenyl ring and LYS180 having distance 1.82 \AA (Fig. 4). ALA286 and VAL283 can form π -alkyl interaction present phenyl ring having bond lengths 4.36 \AA and 4.04 \AA respectively. ASN260 and HIS259 can form hydrogen bonds with methoxy of the compound. There is no significant interaction between mercapto and tyrosinase.

3.5. Acute toxicity

To evaluate acute toxicities of the synthesized compounds, compound **14** was selected to test the acute toxicity. The LD_{50} value for acute toxicity of compound **14** in mice after intragastric administration was obtained. Test result indicated the LD_{50} value of compound **14** was 5000 mg/kg . It showed that compound **14** oral dose commonly used in clinical treatment should be safe. The result might be beneficial to search and develop novel tyrosinase inhibitor with better activity together with lower side effects.

4. Conclusion

In summary, we have developed a series of 1,3,4-thiadiazole derivatives bearing Schiff base moieties as novel tyrosinase inhibitors. The results showed that many of them exhibited remarkable tyrosinase inhibitory activities with IC_{50} values at single digit or sub-micromolar level. Compound **14** was found to be the best tyrosinase inhibitor in this series with the IC_{50} value of $0.036 \mu\text{M}$. Structure-activity relationship (SAR) analysis indicated that (1) free thiol group and hydroxyl group could be active groups in the inhibition; (2) the steric hindrance could be an unfavorable factor; (3) substituted group was introduced onto the benzene ring, an elevated inhibitory activity could be observed; (4) the position and numbers of hydroxyl groups might play an important role in the increase of inhibitory activity. Moreover, the inhibition kinetics study revealed that compounds **13** and **14** exhibited such inhibitory effects on tyrosinase by acting as the uncompetitive inhibitors. Docking studies showed compound **14** combined strongly with mushroom tyrosinase. Hydroxyl group interact with the copper atom of tyrosinase, this result showed that the group was active groups. The acute toxicity of compound **14** was evaluated, LD_{50} value of the compound was 5000 mg/kg . It indicated that compound **14** oral dose commonly used in clinical treatment should be safe.

Acknowledgments

We thank the innovation team of Shaoyang University for funding this project. This work was also financially supported by the Foundation of Education Department of Hunan Province, China (15A172).

References

- [1] R.L.S. Michael, A.R. Christopher, A.R. Patrick, *Bioorg. Med. Chem. Lett.* 21 (2013) 1166–1173.
- [2] Y.C. Li, Y. Wang, H.B. Jiang, J.P. Deng, *Proc. Natl. Acad. Sci. U. S. A.* 106 (2009) 17002–17006.
- [3] Q.X. Chen, X.D. Liu, H. Huang, *Biochemistry (Mosc)* 68 (2003) 644–649.
- [4] X. Dong, Q. Zhu, Y. Dai, J. He, H. Pan, J. Chen, Z.-P. Zheng, *Food Chem.* 192 (2016) 1033–1040.
- [5] R. Matsuura, H. Ukeda, M. Sawamura, *J. Agric. Food Chem.* 54 (2006) 2309–2313.

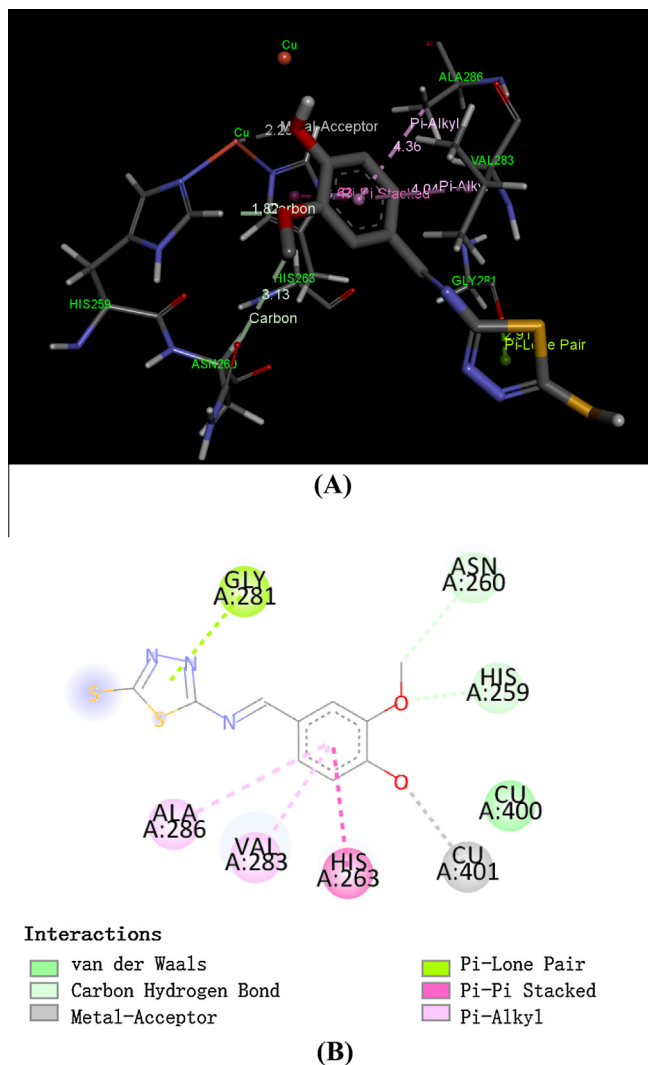


Fig. 4. (A) The interactions of compound (**14**) with the active site of mushroom tyrosinase generated by using AutoDock4.2. It shows the three-dimensional docking of the compound in the binding pocket. Dashed lines indicate bond distances between interacting functionalities of the ligand and receptor. (B) The interactions of compound (**14**) with the active site of mushroom tyrosinase generated by using AutoDock4.2. It shows the two dimensional interaction patterns. The legend inset represents the type of interaction between the ligand atoms and the amino acid residues of the protein.

- [6] C.M. Kumar, U.V. Sathisha, S. Dharmesh, A.G. Rao, S.A. Singh, *Biochimie* 93 (2011) 562–569.
- [7] A. Pinon, Y. Limami, L. Micallef, J. Cook-Moreau, B. Liagre, C. Delage, R.E. Duval, A. Simon, *Exp. Cell Res.* 317 (2011) 1669–1676.
- [8] X. Tan, Y.H. Song, C. Park, K.-W. Lee, J.Y. Kim, D.W. Kim, K.D. Kim, K.W. Lee, *Bioorg. Med. Chem.* 24 (2016) 153–159.
- [9] T. Pan, X. Li, J. Jankovic, *Int. J. Cancer* 128 (2011) 2251–2260.
- [10] Y.J. Zhu, H.T. Zhou, Y.H. Hu, *Food Chem.* 124 (2011) 298–302.
- [11] F. Artés, M. Castañer, M.I. Gil, *Food Sci. Technol. Int.* 4 (1998) 377–389.
- [12] M. Ashida, P. Brey, *Proc. Natl. Acad. Sci. U.S.A.* 92 (1995) 10698–10702.
- [13] A. Ortiz-Urquiza, N.O. Keyhani, *Insects* 4 (2013) 357–374.
- [14] Y. Mu, L. Li, S.Q. Hu, *Spectrochim. Acta A. Mol. Biomol. Spectrosc.* 107 (2013) 235–240.
- [15] P. Han, C. Chen, C. Zhang, K. Song, H. Zhou, Q. Chen, *Food Chem.* 107 (2008) 797–803.
- [16] M.T.H. Khan, *Curr. Med. Chem.* 19 (2012) 2262–2272.
- [17] I.E. Orhan, M.T.H. Khan, *Curr. Top Med. Chem.* 14 (2014) 1486–1493.
- [18] L. Xia, A. Idhayadhulla, Y.R. Lee, Y.J. Wee, S.H. Kim, *Eur. J. Med. Chem.* 86 (2014) 605–612.
- [19] A. You, J. Zhou, S. Song, G. Zhu, H. Song, W. Yi, *Bioorg. Med. Chem.* 23 (2015) 924–931.
- [20] G. Battaini, E. Monzani, L. Casella, L. Santagostini, R. Pagliarin, *J. Biol. Inorg. Chem.* 5 (2000) 262–268.
- [21] H.R. Kim, H.J. Lee, Y.J. Choi, Y.J. Park, *Med. Chem. Commun.* 5 (2014) 1410–1417.
- [22] T. Klabunde, C. Eicken, J.C. Sacchetti, B. Krebs, *Nat. Struct. Biol.* 5 (1998) 1084–1090.
- [23] A. You, J. Zhou, S. Song, G. Zhu, H. Song, W. Yi, *Eur. J. Med. Chem.* 93 (2015) 255–262.
- [24] N. Grynberg, A.C. Santos, A. Echevarria, *Anticancer Drugs* 8 (1997) 88–91.
- [25] A. Senff-Ribeiro, A. Echevarria, E.F. Silva, C.R. Franco, S.S. Veiga, M.B. Oliveira, *Br. J. Cancer* 91 (2004) 297–304.
- [26] Z. Luo, B. Chen, S. He, Y. Shi, Y. Liu, C. Li, *Bioorg. Med. Chem. Lett.* 22 (2012) 3191–3193.
- [27] N. Polkam, P. Rayam, J.S. Anireddy, S. Yennam, H.S. Anantaram, S. Dharmarajan, *Bioorg. Med. Chem. Lett.* 25 (2015) 1398–1402.
- [28] S.-J. Yang, S.-H. Lee, H.-J. Kwak, Y.-D. Gong, *J. Org. Chem.* 78 (2013) 438–444.
- [29] T.A. Farghaly, M.A. Abdallah, G.S. Masaret, Z.A. Muhammad, *Eur. J. Med. Chem.* 97 (2015) 320–333.
- [30] K. Zhang, P. Wang, L.-N. Xuan, X.-Y. Fu, F. Jing, S. Li, Y.-M. Liu, B.-Q. Chen, *Bioorg. Med. Chem. Lett.* 24 (2014) 5154–5156.
- [31] A. Skrzypek, J. Matysiak, A. Niewiadomy, M. Bajda, P. Szymanski, *Eur. J. Med. Chem.* 62 (2013) 311–319.
- [32] H.-C. Zhao, Y.-P. Shi, Y.-M. Liu, C.-W. Li, L.-N. Xuan, P. Wang, K. Zhang, B.-Q. Chen, *Bioorg. Med. Chem. Lett.* 23 (2013) 6577–6579.
- [33] J. Xie, H. Dong, Y. Yu, S. Cao, *Food Chem.* 190 (2016) 709–716.
- [34] U. Ghani, N. Ullah, *Bioorg. Med. Chem.* 18 (2010) 4042–4048.
- [35] M. Yusuf, R.A. Khan, B. Ahmed, *Bioorg. Med. Chem.* 16 (2008) 8029–8034.
- [36] J.B. Liu, W. Yi, Y.Q. Wan, L. Ma, H.C. Song, *Bioorg. Med. Chem.* 16 (2008) 1096–1102.
- [37] Y.-H. Hu, X. Liu, Y.-L. Jia, Y.-J. Guo, Q. Wang, Q.-X. Chen, *J. Biosci. Bioeng.* 117 (2014) 142–146.
- [38] Z. Ashraf, M. Rafiq, S.-Y. Seo, K.S. Kwon, M.M. Babar, *Eur. J. Med. Chem.* 98 (2015) 203–211.
- [39] Y. Matoba, T. Kumagai, A. Yamamoto, H. Yoshitsu, M. Sugiyama, *J. Biol. Chem.* 281 (2006) 8981–8990.
- [40] S. Radhakrishnan, R. Shimmon, C. Conn, A. Baker, *Bioorg. Chem.* 63 (2015) 116–122.
- [41] J. Liu, F. Wu, H. Song, H. Wang, L. Zhao, *Med. Chem. Res.* 22 (2013) 4228–4238.
- [42] S. Li, Y. Xue, H. Zhang, H. Nie, L. Zhu, *Fine Chem.* 26 (2009) 889–893.